Quartz crystal microbalance for real-time monitoring chlorosilane gas transport in slim vertical cold wall chemical vapor deposition reactor

Toshinori Takahashi[1], Mana Otani[1], Mitsuko Muroi[1], Kenta Irikura[1], Miya Matsuo[1], Ayami Yamada[1], Hitoshi Habuka[1], Yuuki Ishida[2, 3], Shin-Ichi Ikeda[2, 3] and Shiro Hara[2, 3]

[1] Yokohama National University, Yokohama, Japan

[2] National Institutes of Advanced Science and Technology, Tsukuba, Japan

[3] Minimal Fab Development Association, Tsukuba, Japan

Chlorosilane gas transport in ambient hydrogen in a slim vertical cold wall chemical vapor deposition reactor was real-time monitored using a quartz crystal microbalance (QCM) using its behaviour responding to the properties of the gas mixture. The QCM frequency quickly decreased by introducing the trichlorosilane gas, while it slowly decreased by the dichlorosilane gas. The QCM frequency behavior was explained by the gas flow condition, such as the plug flow and recirculating flow, in the reactor. The relationship was consistent with the gas flow calculations, because the heavy and light gases could directly flow downward and recirculate, respectively, in the chamber due to natural convection. The information obtained from the QCM frequency behavior is expected to be utilized for the real-time gas monitoring and for the process design.

Keywords: Minimal Fab, chemical vapor deposition reactor, quartz crystal microbalance, silicon epitaxial growth, trichlorosilane, dichlorosilane

1. Introduction

In order to improve the quality, safety, and productivity of film formation during the Chemical Vapor Deposition (CVD), the process sequence and time for utilizing various gases should be carefully and finely designed. Specifically, the details for controlling the arrival and purge of the gases are expected to be real-time monitored.

As the process monitoring tool for scientific purposes, quadruple mass spectrometry (QMS) and infrared (IR) light absorption spectroscopy have been used [1-6]. In order to significantly improve the industrial manufacturing system and process control, taking into account the concept of the Internet of Things (IoT) [7, 8], the real-time monitoring devices are expected to be installed at multiple monitoring points while achieving a reasonable cost. The process control requires real-time information about the gas flowing through many parts of the system, such as the gas cylinder, the mass flow controllers for the precursors, the gas inlet, the gas exhaust and the waste gas cleaner. For example, the arrival time of each precursor at the inlet should be finely controlled. Additionally, the time of film formation can be finely controlled, if the real-time monitoring of the gas condition at the inlet was possible. Furthermore, the characteristic gas transport in the chamber is expected to be obtained by means of comparing the real-time gas concentration increase and decrease between the inlet and outlet. However, an applicable real-time monitoring tool has not been studied.

One of the manufacturing systems for real-time monitoring is the Minimal Fab [9-13]. This is the semiconductor device manufacturing system based on the quick process developed for the small wafers with a half-inch diameter. In order to make the Minimal CVD process fast as

possible, the multiple-point monitoring technique by small and reasonable-cost sensors is expected.

For this purpose, a piezoelectric crystal microbalance [14-18], such as a quartz crystal microbalance (QCM), was considered. The QCM is a simple, small and low-cost sensor. It could sensitively detect various phenomena that occurred related to the CVD process, such as the gas density and viscosity change in the reactor in addition to the deposition on the surface [14-17]. In the first study applying the QCM to the Minimal CVD system [18], the gas property change and the byproduct deposition at the exhaust of the reactor were studied relating to the silicon film deposition in a trichlorosilane-hydrogen system.

For developing the real-time monitoring technique for the Minimal CVD, the QCM system should be further studied for obtaining transient information about the gas transport. A suitable example to be verified is the gas transport difference between the gas precursors, such as the trichlorosilane ($SiHCl_3$) and dichlorosilane (SiH_2Cl_2). Both of them are the major precursors for the silicon film formation. While producing a similar chemical reaction, they have different gas densities, which may govern the gas transport condition, such as that related to natural convection in a vertical gas channel.

This study used the QCM sensors placed at the inlet and the exhaust tube of a slim vertical cold wall CVD reactor for the Minimal Fab. in order to extend the application of the real-time monitoring technique. The transport characteristics of the trichlorosilane and dichlorosilane gases in ambient hydrogen (H_2) were focused on.

2. Experimental procedure

Figure 1 shows the slim vertical cold wall CVD reactor used in this study. A half-inch-diameter silicon wafer was placed at the center position of the slim vertical quartz tube. The wafer was heated by infrared light through the transparent quartz tube coming from three halogen lamps. The wafer was rotated at the rate of 4-10 rpm. The trichlorosilane and dichlorosilane gases were used as the precursors in order to form the silicon epitaxial film on the silicon wafer surface. The precursor gases were added to the ambient hydrogen at atmospheric pressure from the gas inlet situated on top of the reactor. The overall chemical reactions are assumed as follows:

$$SiHCl_3 + H_2 \rightarrow Si + 3HCl \quad (1)$$

$$SiH_2Cl_2 \rightarrow Si + 2\,HCl \quad (2)$$

These gases passed over the QCM sensor surface in the QCM box, as shown in Figure 1 (b). The QCM box placed at the inlet, as shown in Figure 1 (a), measured the gases before causing any chemical reactions. The gases after these reactions were again measured by the QCM box placed at the exhaust position. The exhaust gases could be sufficiently cooled to room temperature before arriving at the QCM sensor so that the QCM frequency in this study was influenced by the gas properties and the byproduct deposition, and not by the wafer and gas temperatures changing in the quartz tube. The QCM frequency (25 MHz) was measured and recorded by a personal computer.

The silicon film deposition was performed following the process shown in Figure 2. The silicon wafer surface was first cleaned at temperatures higher than 1000 ^{o}C in ambient hydrogen between Steps A and B for one minute. The native oxide and organic contaminations present on the silicon wafer surface were removed. During Step B, the silicon wafer temperature was decreased to a sufficiently low value to have no reaction with the trichlorosilane and dichlorosilane gases. After adding the trichlorosilane or dichlorosilane gas at Step C, the wafer temperature was again increased at Step D to that of the silicon epitaxial film formation. The chlorosilane gases arrived at the reactor after going through the gas tube when the wafer temperature reached that for the epitaxial film formation. In this study, the concentrations of the trichlorosilane and dichlorosilane gases were 10 - 20 % in the ambient hydrogen. The total gas flow rate was about 100 sccm. Taking into account the time for the precursors to approach and go through the reactor chamber, the duration for the silicon film deposition was about one minute. The epitaxial growth rate was evaluated by the increase in the thickness and weight of the wafer.

The influences of various CVD parameters and phenomena on the QCM frequency are briefly explained and shown in Figure 3. Because the trichlorosilane and dichlorosilane gases are heavier and more viscous than the ambient hydrogen, the QCM frequency was assumed to decrease following the change in the density (ρ) and viscosity (μ) of the gas mixture based on the experiment reported in a previous study [15].

$$\text{QCM frequency change} \propto (\rho \times \mu)^{1.3} \tag{3}$$

Such a gas property change immediately occurs corresponding to the arrival of the precursor gas and can be distinguished using the slope of the QCM frequency change, as shown in Fig. 3. The QCM frequency is simultaneously influenced by the weight increase, Δw, due to any deposition on the QCM sensor surface. Because such a weight change was generally slower than the gas property change, it tends to appear after the gas property change. Thus, the gradual and continuous QCM frequency decrease that occurred after the quick decrease could be distinguished and assigned to the deposition of the byproduct.

This study focused on the gas property change. The quick QCM frequency change for about 20 - 50 seconds after starting the decrease was compared and evaluated between the trichlorosilane and the dichlorosilane.

The dichlorosilane gas behaviour was observed in this study. The measurement and calculation of the trichlorosilane gas transport behaviour obtained in previous studies [18, 19] were further evaluated and compared with that of dichlorosilane gas.

3. Results and discussion

3.1 QCM frequency behaviour

The QCM frequency behaviour was measured at the inlet and exhaust of the reactor. After the arrival of the dichlorosilane gas at a concentration of 10 %, the QCM frequency at the inlet quickly decreased for about 20 seconds, as shown in Figure 4.

The QCM frequency was next measured at the exhaust and shown in Figure 5 when the silicon epitaxial growth rate was 0.7 $\mu m\ min^{-1}$ by the process shown in Figure 2. As predicted by

the preliminary evaluation [18], the QCM frequency was not influenced by any temperature change in the quartz tube. Actually, in Figure 5, the QCM frequency did not change between Steps A and C.

The time of the trichlorosilane and dichlorosilane gases arriving at the QCM surface was indicated as zero seconds in Figure 5. In the trichlorosilane-hydrogen system, the QCM frequency suddenly started decreasing at zero seconds. Such a frequency decrease from 0 to -1000 Hz was considered to be due to the quick gas property change from the hydrogen to the gas mixture containing the trichlorosilane. The quick QCM frequency decrease continued for about 20 seconds. This indicated the arrival of the trichlorosilane at the QCM. After 20 seconds, the QCM frequency still continued decreasing, but the slope became very gradual. This could be due to the byproduct deposition, as shown in Figure 3.

Figure 5 simultaneously shows the QCM frequency behavior in the dichlorosilane-hydrogen system. The QCM frequency decrease between 0 and 20 seconds in this system was clearly slower than that in the trichlorosilane-hydrogen system. At the dichlorosilane gas concentration of 20 %, the QCM frequency started to decrease at zero seconds, similar to the trichlorosilane gas. The QCM frequency decreased from 0 Hz to about -200 Hz for about 50 seconds. At nearly 50 seconds, the slope of the QCM frequency became moderate. At 300 seconds after the continuous QCM frequency decrease, the QCM frequency became nearly -500 Hz. Overall, the change in the QCM frequency at the dichlorosilane gas concentration of 20% was more moderate than that at the trichlorosilane gas concentration of 20%. For example, the drop in the QCM frequency at zero seconds was slow and shallow in the

dichlorosilane-hydrogen system. This shallow drop was due to the small decrease in the $(\rho\mu)^{1.3}$ value. Specifically, because the molecular weight of the dichlorosilane, 101, is lower than that of the trichlorosilane, 135.5, the QCM frequency drop at zero seconds was quite small in the dichlorosilane-hydrogen system. At the dichlorosilane gas concentration of 10 %, the QCM frequency decrease between 0 and 50 seconds became even further slower because of the fewer decrease in the average molecular weight of the gas mixture.

The depth of the QCM frequency drop, being deep and shallow at zero seconds, could be clearly and theoretically related to the average molecular weight of the gas mixture. In contrast, the slope of the QCM frequency drop initiated at zero seconds, being quick and slow, could be caused by a different mechanism, such as the flowing gas.

3.2 Gas density and gas flow

The average molecular weight of the gas mixture, MW_{ave} (-), is considered to significantly affect the natural convection in the vertical gas channel [20]. Thus, the gas movements at various average molecular weights were studied, accounting for the calculations of the gas flow at the wafer temperature of 1000 ^{o}C in the trichlorosilane-hydrogen system [19]. For the gas mixture containing 20% trichlorosilane gas in the ambient hydrogen, the MW_{ave} value was 28.7. At the 10 and 20% dichlorosilane gas concentrations in the ambient hydrogen, the MW_{ave} values were 11.9 and 21.8, respectively.

Taking into account the MW_{ave} value, the gas flows and the gas temperatures in the slim vertical gas channel were studied, as shown in Figures 6 and 7. The temperature distribution was

also evaluated for easily determining the influence of gas flow.

Figure 6 shows the gas flows at the MW_{ave} values of (a) 8.7, (b) 15.3 and (c) 28.7, corresponding to the trichlorosilane gas concentrations of 5, 10 and 20%, respectively. The gas flows for the MW_{ave} value at the 10 % dichlorosilane gas concentration are considered to be that between Figures 6 (a) and (b). Similarly, the gas flows for the MW_{ave} value at the 20 % dichlorosilane gas concentration are assumed to be those between Figures 6 (b) and (c). The MW_{ave} value of Figures 6 (a), (b) and (c) are the same as the temperature distribution in Figures 7 (a), (b) and (c), respectively.

As shown in Figure 6 (a), the upward gas flow from the wafer surface is dominant at the low MW_{ave} values, because of the high natural convection rising from the hot wafer surface. As shown in Figure 7 (a), the high temperature region is extended to a very high position above the wafer. A tall region of high temperatures was formed due to the upward gas flow rising from the hot wafer surface, as shown in Figure 6 (a).

With the increasing MW_{ave} values, the upward motions tend to be suppressed, as shown in Figure 6 (b). In this figure, the upward gas flow seems to be limited to near the hot wafer surface. Thus, the hot temperature region shrunk, as shown in Figure 7 (b), because the upward flow becomes weak corresponding to the increase in the gas density.

At the high MW_{ave} value for the 20% trichlorosilane gas concentration, the gas mixture injected from the reactor top flows directly downward to the wafer surface, as shown in Figure 6 (c). Figure 7 (c) shows that the high temperature region is significantly suppressed near the wafer surface by the gas mixture having the high MW_{ave} value. Taking into account the gas flows

shown in Figure 6 (c), the cold gas coming from the top of the slim vertical gas channel directly flows downward to the wafer surface to cool the gas phase.

The gas flow paths in the slim vertical gas channel are schematically summarized and shown in Figure 8. In this figure, the hatched region indicates that the chlorosilane gas arrived. (I) and (II) show the flows of heavy and light gas mixtures, respectively. The chlorosilane gas advances following (a), (b), (c) and (d). Figure 8 (e) is the typical QCM frequency behaviour.

As shown in Figures 8 (I)-(a), (b), (c) and (d), the heavy gas supplied from the top of the very slim gas channel goes quickly straight downward to approach the wafer surface. Such a gas flow is recognized to be plug flow. The low temperature region is extended from the top of the chamber to the space near the wafer surface. The heavy gas quickly goes through the bottom of the reactor to reach the QCM, purging the hydrogen gas present. Thus, the heavy gas was not mixed with the hydrogen gas. Following the gas flow shown in Figure 8 (I), the QCM frequency at the trichlorosilane gas concentration of 20 % showed a quick decrease from 0 to about -1000 Hz within 20 seconds, as shown in Figures 5 and 8 (I)-(e).

In contrast, at the low dichlorosilane concentrations, the light gas moves with a strong upward flow and recirculation due to natural convection, as shown in Figures 8 (II)-(a), (b), (c) and (d). The dichlorosilane gas supplied from the top of the reactor chamber is considered to be indirectly transported to the wafer surface following the gas recirculation. The chlorosilane gas is mixed with the hydrogen gas above the hot wafer surface. Along with accompanying such a mixing, the chlorosilane gas goes through the bottom of the reactor to reach the QCM. Thus, the dichlorosilane gas concentration gradually increases at the exhaust. The QCM frequency in the

dichlorosilane-hydrogen system showed a slow decrease, as shown in Figures 5 and 8 (II)-(e). Consequently, the difference in the gas transport, such as the plug flow and the recirculating flow, could be real-time monitored and identified by the quick and slow, respectively, QCM frequency decrease.

4. Conclusions

The gas flow condition and the temperature distribution from the inlet to the outlet of the CVD reactor, influencing the thin film deposition, were studied, based on the information obtained by the QCM sensors set at the inlet and outlet of the CVD reactor.

The QCM measurement was performed for the silicon epitaxial growth from the trichlorosilane and dichlorosilane gases in ambient hydrogen using the slim vertical cold wall CVD reactor for the Minimal Fab. The QCM frequency behaviour responding to the properties of the gas mixture was utilized. Although the QCM frequency measured at the inlet quickly decreased for about 20 seconds, that at the exhaust was different from that at the inlet. The QCM frequency quickly decreased by introducing the heavy gas, trichlorosilane, while it slowly decreased by introducing the light gas, dichlorosilane. This difference was consistent with the gas flow and heat calculations which explained the plug flow and recirculating flow that occurred due to the heavy gas and the light gas, respectively, in the reactor. The QCM is expected to real-time detect, distinguish and assign the gas transport condition.

Acknowledgement

The authors thank Mr. Nobuyoshi Enomoto and Mr. Hitoshi Ueno of Halloran Electronics Co., Ltd., for their helpful suggestions and support.

References

[1] A. A. Puretzky, D. B. Geohegan, S. Jesse, I. N. Ivanov and G. Eres, In Situ Measurements and Modeling of Carbon Nanotube Array Growth Kinetics During Chemical Vapor Deposition, Applied Physics A, 81 (2), 223–240 (2005).

[2] S. Nakamura, In Situ Monitoring of GaN Growth Using Interference Effects, Jap. J. Appl. Phys., 30 (8), 1620-1628 (1971).

[3] L. L. Tedder and G. W. Rubloff, Real‐Time Process and Product Diagnostics in Rapid Thermal Chemical Vapor Deposition Using In Situ Mass Spectrometric Sampling, J. Vac. Sci. Technol. B, 13, 1924 (1995).

[4] H. Habuka, Y. Aoyama, S. Akiyama, T. Otsuka, W. F. Qu, M. Shimada and K. Okuyama, Chemical Process of Silicon Epitaxial Growth in a $SiHCl_3$-H_2 System, J. Crystal Growth, 207(1), 77-86 (1999).

[5] F. G. Celii, Direct Monitoring of CH_3 in a Filament‐Assisted Diamond Chemical Vapor Deposition Reactor, J. Appl. Phys., 71, 2877 (1992).

[6] H. Fujiwara. and M. Kondo, Real-Time Monitoring and Process Control in Amorphous⁄Crystalline Silicon Heterojunction Solar Cells by Spectroscopic Ellipsometry and Infrared Spectroscopy, Appl. Phys. Lett. 86, 032112 (2005).

[7] L. Atzori, A. Iera and G. Morabito, The Internet of Things: A survey, Computer Networks, 54 (15), 2787-2805 (2010).

[8] J. Gubbi, R. Buyya, S. Marusic and M. Palaniswami, Internet of Things (IoT): A Vision, Architectural Elements, and Future Directions, Future Generation Computer Systems, 29 (7),

1645-1660 (2013).

[9] S. Khumpuang, S. Maekawa, and S. Hara, Photolithography for Minimal Fab System, IEEJ Trans. Sensors and Micromachines,133, 272-277 (2013).

[10] S. Khumpuang, F. Imura and S. Hara, Analyses on Cleanroom-Free Performance and Transistor Manufacturing Cycle Time of Minimal Fab, IEEE Trans. Semicond. Manufac., 28 (4), 551-556 (2015).

[11] N. Li, H. Habuka, S. Ikeda and S. Hara, Silicon Chemical Vapor Deposition Process Using a Half-Inch Silicon Wafer for Minimal Manufacturing System, Physics Procedia, 46, 230-238 (2013).

[12] N. Li , H. Habuka, Y. Ishida , S. Ikeda and S. Hara, Reflector Influence on Rapid Heating of Minimal Manufacturing Chemical Vapor Deposition Reactor, ECS J. Solid State Sci. Technol., 5 (5), P280-P284 (2016).

[13] A. Yamada, N. Li, M. Matsuo, M. Muroi, H. Habuka, Y. Ishida, S. Ikeda and S. Hara, Transport Phenomena in a Slim Vertical Atmospheric Pressure Chemical Vapor Deposition Reactor Utilizing Natural Convection, Mater. Sci. Semicond. Processing, 71, 348-351 (2017).

[14] K. Miyazaki, A. Saito and H. Habuka, In Situ Measurement for Evaluating Temperature Change Related to Silicon Film Formation in a $SiHCl_3$-H_2 System, ECS J Solid State Sci. Technol., 5 (2), P16-P20 (2016).

[15] H. Habuka and M. Matsui, Langasite Crystal Microbalance Frequency Behavior over Wide Gas Phase Conditions for Chemical Vapor Deposition, Surf. Coat. Technol., 230, 312-315 (2013).

[16] H. Habuka and Y. Tanaka, In-Situ Monitoring of Chemical Vapor Deposition from Trichlorosilane Gas and Monomethylsilane Gas Using Langasite Crystal Microbalance, J. Surface Eng. Materi. Adv. Technol.,3, 61-66 (2013).

[17] H. Habuka and Y. Tanaka, Langasite Crystal Microbalance Used for In-Situ Monitoring of Amorphous Silicon Carbide Film Deposition, ECS J. Solid State Sci. Technol., 1(2), 62-65 (2012).

[18] M. Muroi, M. Matsuo, H. Habuka, Y.Ishida, S. Ikeda and S. Hara, Real Time Evaluation of Silicon Epitaxial Growth Process by Exhaust Gas Measurement Using Quartz Crystal Microbalance, Materi. Sci. Semicond. Process., 88, 192-197 (2018).

[19] K. Irikura, M. Muroi, A. Yamada, M. Matsuo, H. Habuka, Y. Ishida, S. Ikeda and S. Hara, Advantages of a Slim Vertical Gas Channel at High $SiHCl_3$ Concentrations for Atmospheric Pressure Silicon Epitaxial Growth, Mater. Sci. Semicond. Process., 87, 13-18 (2018).

[20] R. B. Bird, W. E. Stewart and E. N. Lightfoot, Transport Phenomena, 2nd Ed. John Wiley and Sons (2007).

Figure captions

Figure 1 Chemical vapor deposition reactor having the QCM sensor as a real-time monitoring system. (a) the reactor and (b) the QCM box.

Figure 2 Silicon epitaxial growth consisting of two separated processes, *i.e.*, wafer surface cleaning and silicon epitaxial growth.

Figure 3 QCM frequency behavior influenced by gas ambient and deposition on surface.

Figure 4 Quartz crystal microbalance frequency behavior measured when the 10 % SiH_2Cl_2 gas arrived at the QCM box set at the inlet.

Figure 5 Quartz crystal microbalance frequency behavior measured at the exhaust of the reactor during silicon epitaxial film deposition using $SiHCl_3$ and SiH_2Cl_2.

Figure 6 Gas motions at the MW_{ave} values of (a) 8.7, (b) 15.3 and (c) 28.7.

Figure 7 Contour diagram of gas phase temperature at the MW_{ave} values of (a) 8.7, (b) 15.3 and (c) 28.7.

Figure 8 Schematic of gas flow in vertical cold wall reactor. (I) Heavy gas mixture and (II) light gas mixture. Hatched region: chlorosilane gas position. (a), (b), (c) and (d): chlorosilane gas advance, and (e): QCM frequency behaviour.

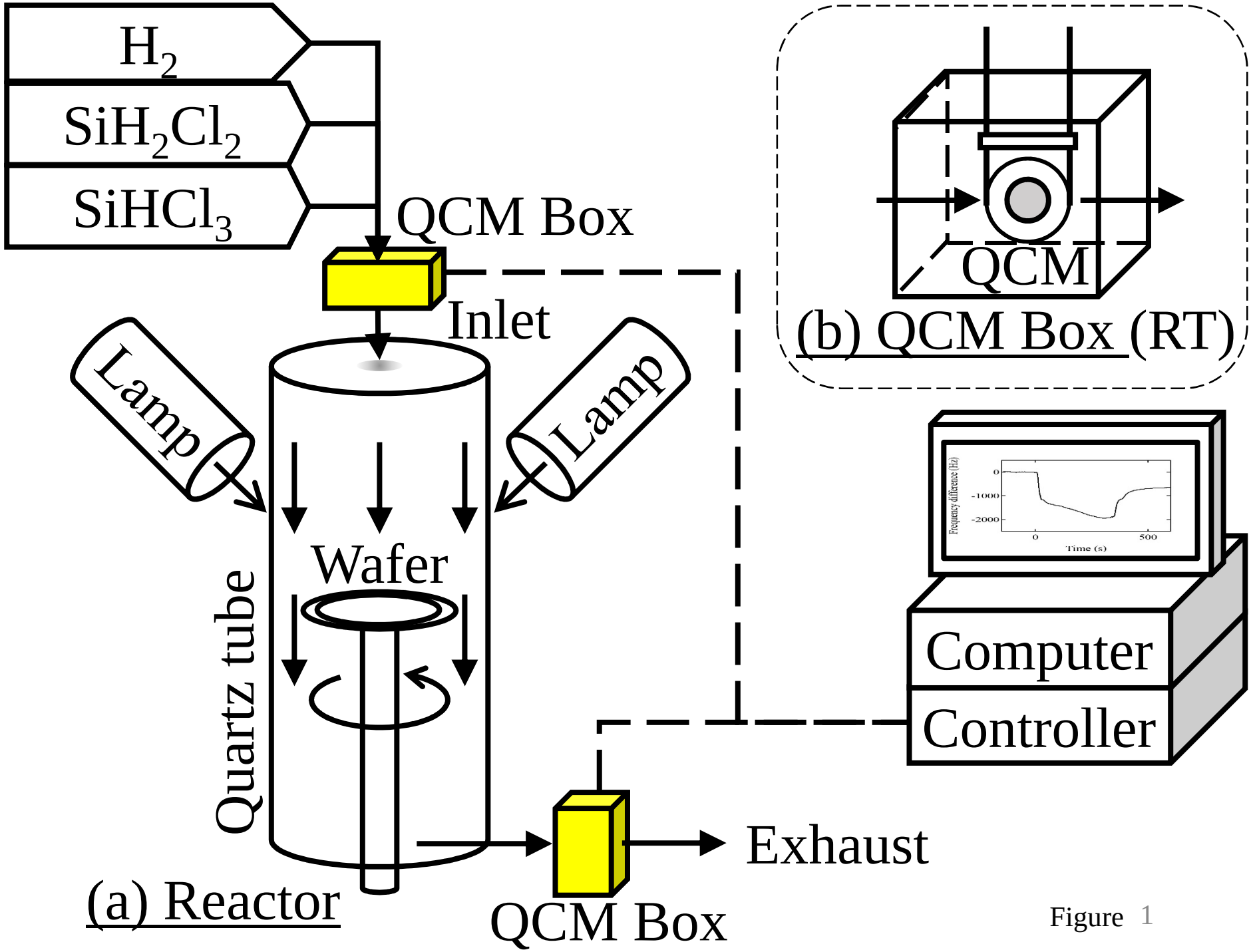
H_2
SiH_2Cl_2
$SiHCl_3$
QCM Box
Inlet
Lamp
Lamp
Wafer
Quartz tube
(a) Reactor
QCM Box
Exhaust
QCM
(b) QCM Box (RT)
Frequency difference (Hz)
0
-1000
-2000
0
500
Time (s)
Computer
Controller

Figure 1

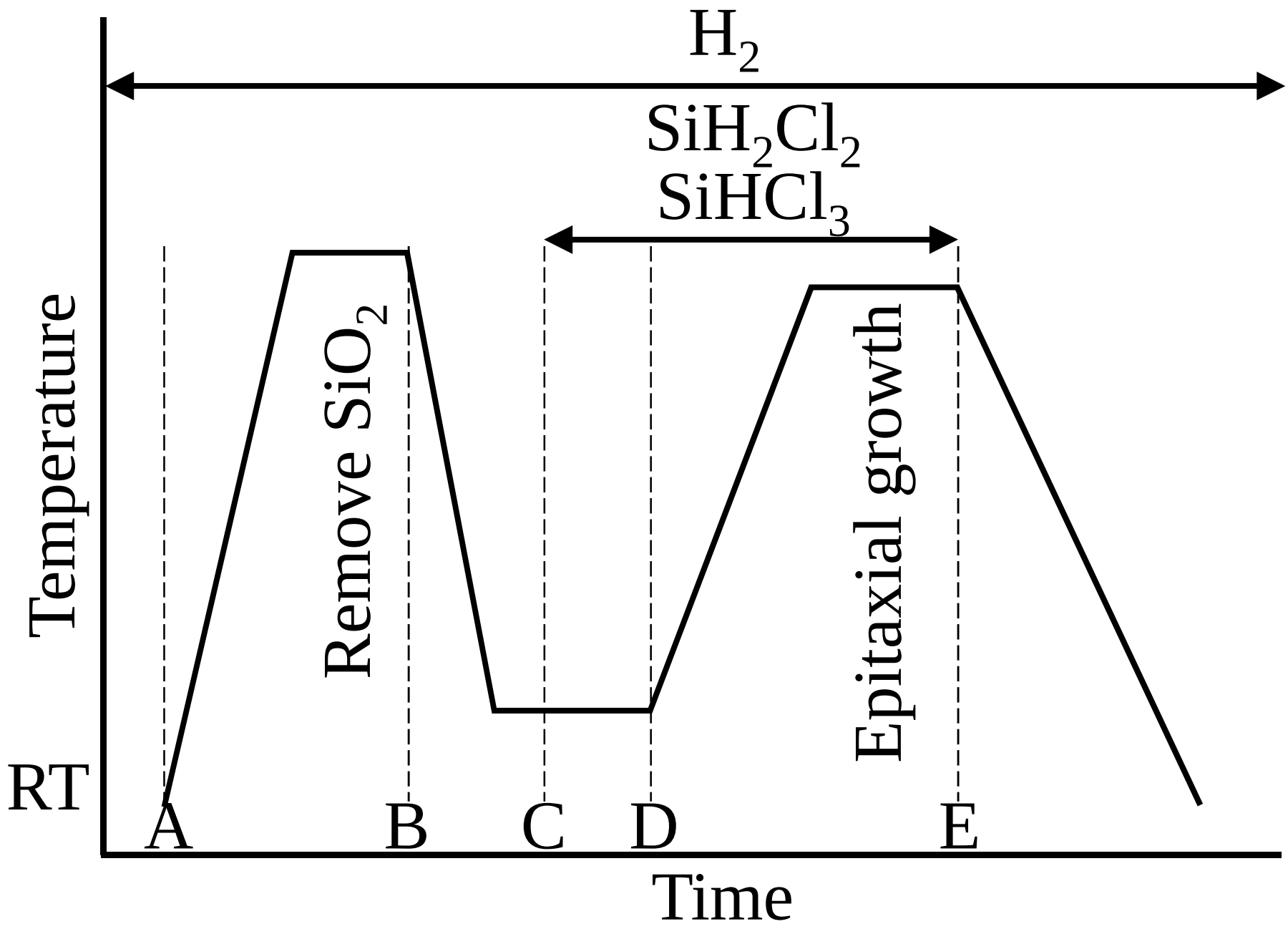
H2
SiH2Cl2
SiHCl3
Temperature
Remove SiO2
Epitaxial growth
RT
A
B
C
D
E
Time

Figure 2

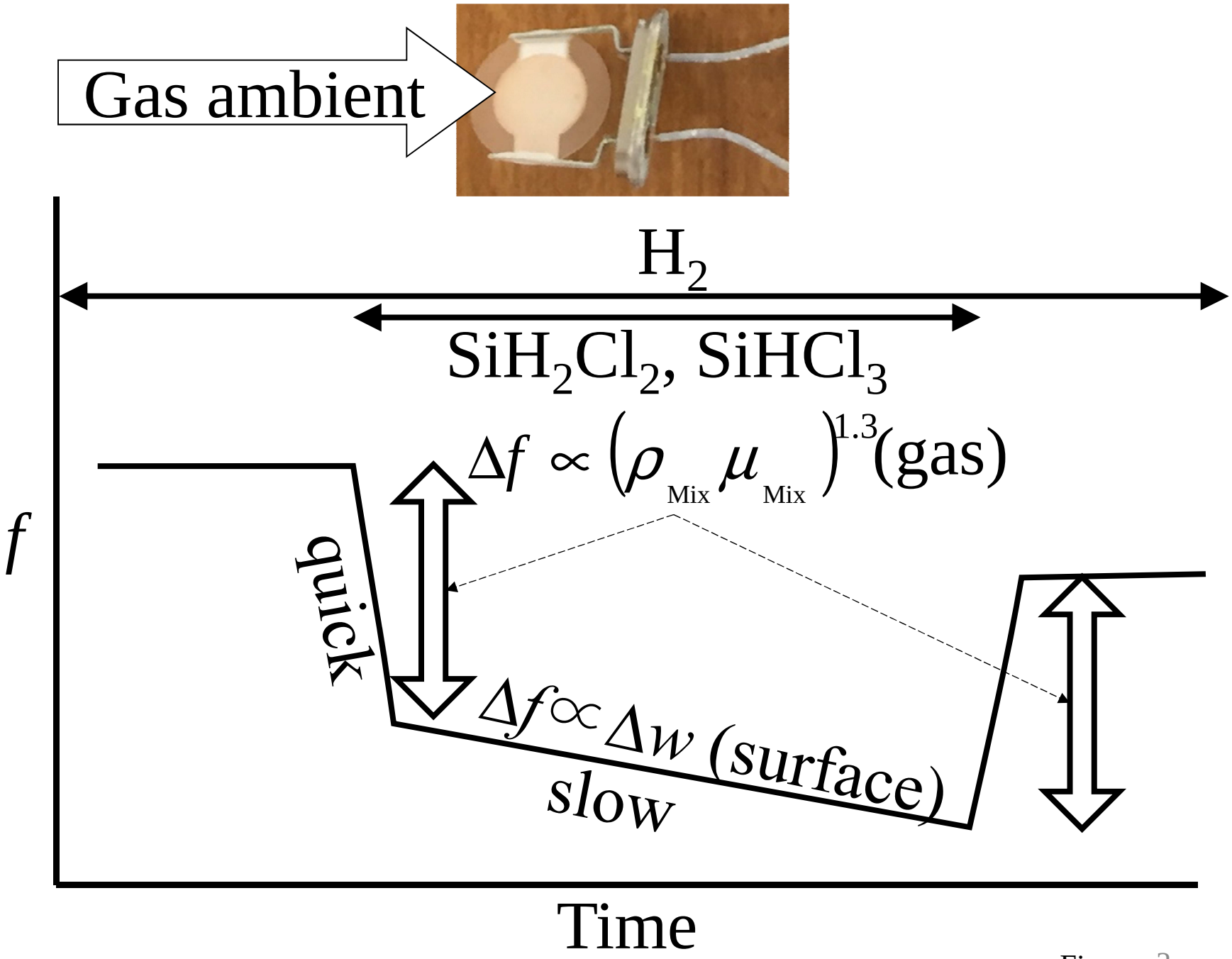
Gas ambient
H2
SiH2Cl2, SiHCl3
Δf ∝ (ρMix μMix)1.3(gas)
f
quick
Δf∝Δw (surface)
slow
Time

Figure 3

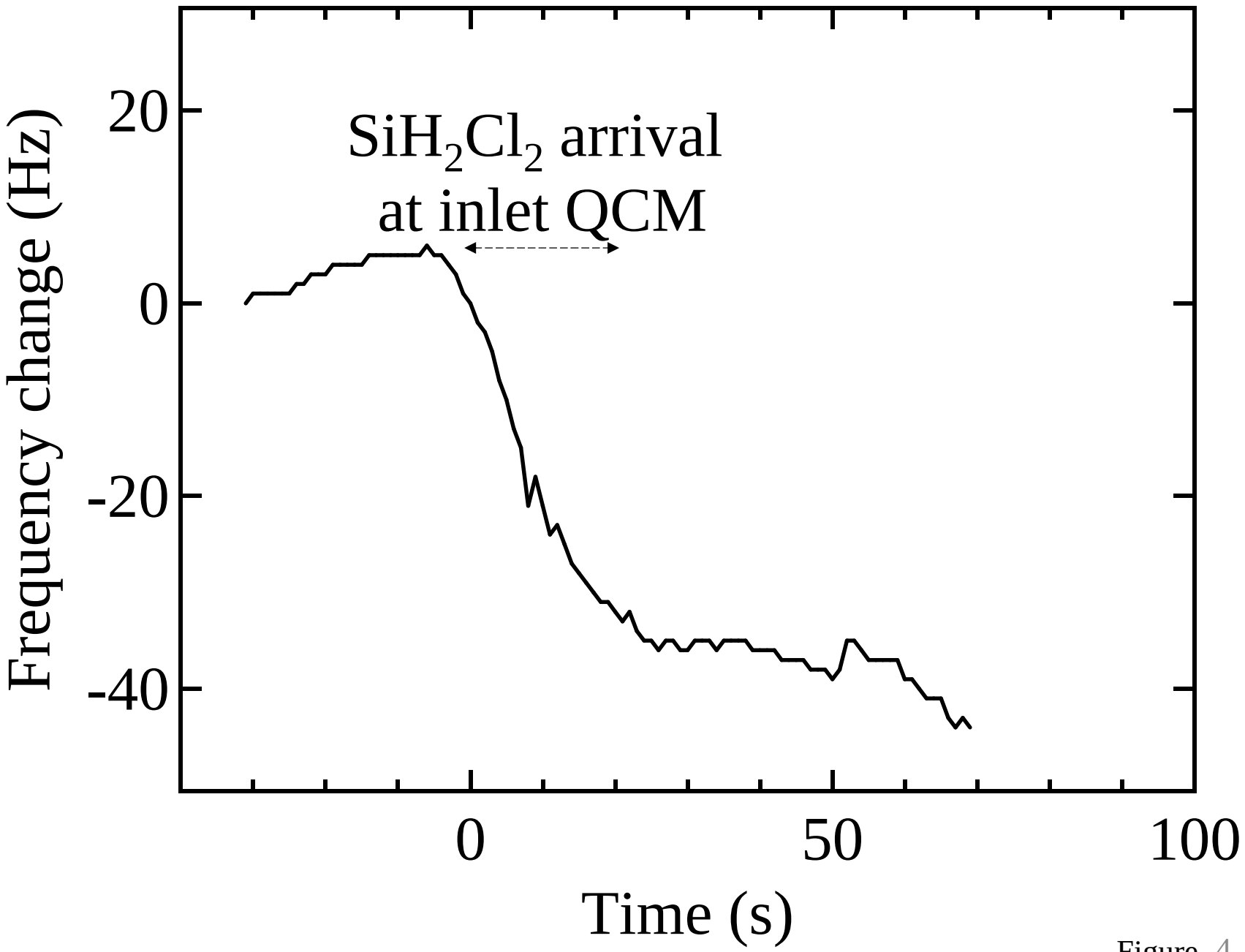
Frequency change (Hz)
20
0
-20
-40
SiH2Cl2 arrival
at inlet QCM
0
50
100
Time (s)

Figure 4

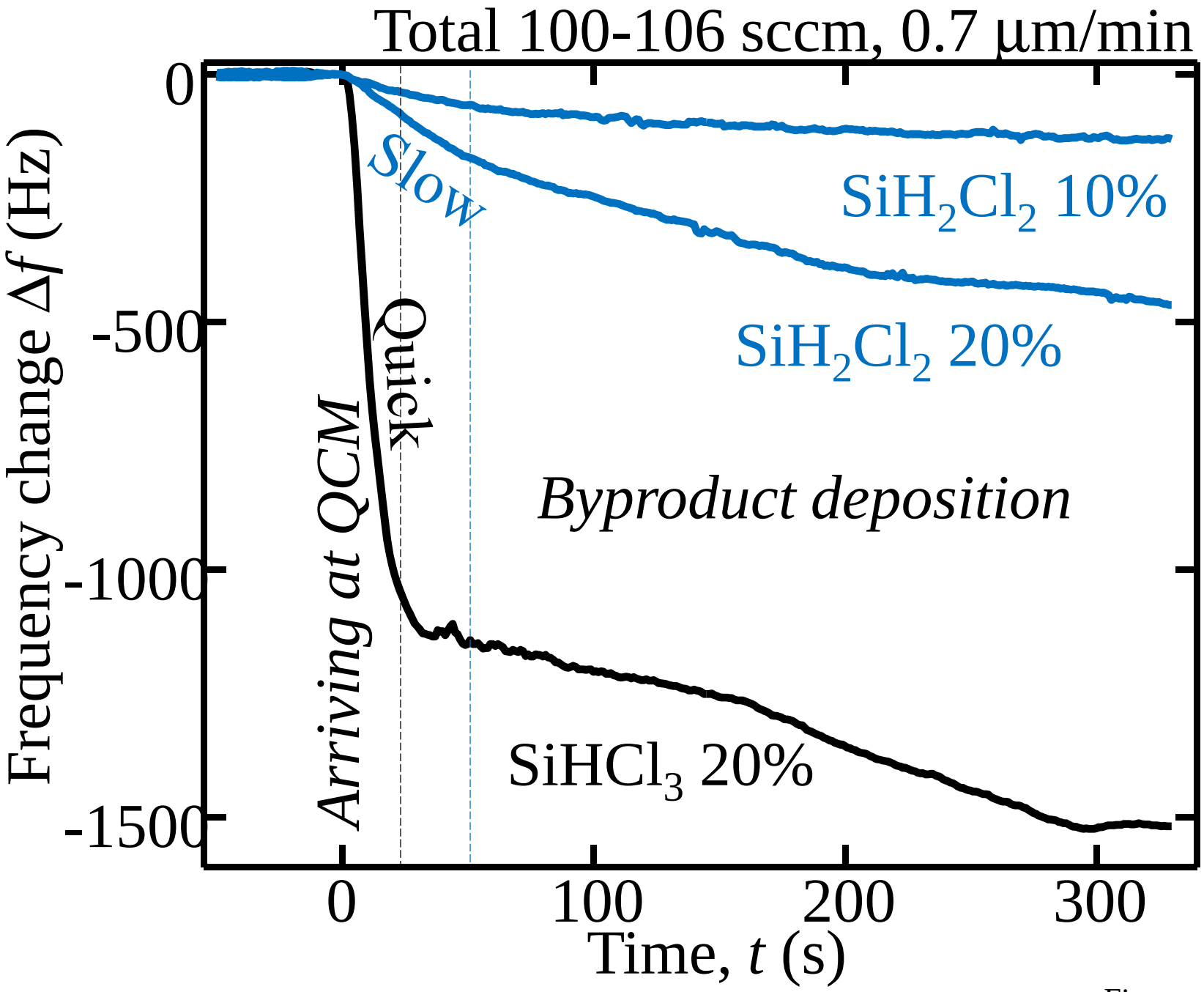
Total 100-106 sccm, 0.7 μm/min
Frequency change Δf (Hz)
0
-500
-1000
-1500
0
100
200
300
Time, t (s)
Slow
Quick
Arriving at QCM
SiH2Cl2 10%
SiH2Cl2 20%
Byproduct deposition
SiHCl3 20%

Figure 5

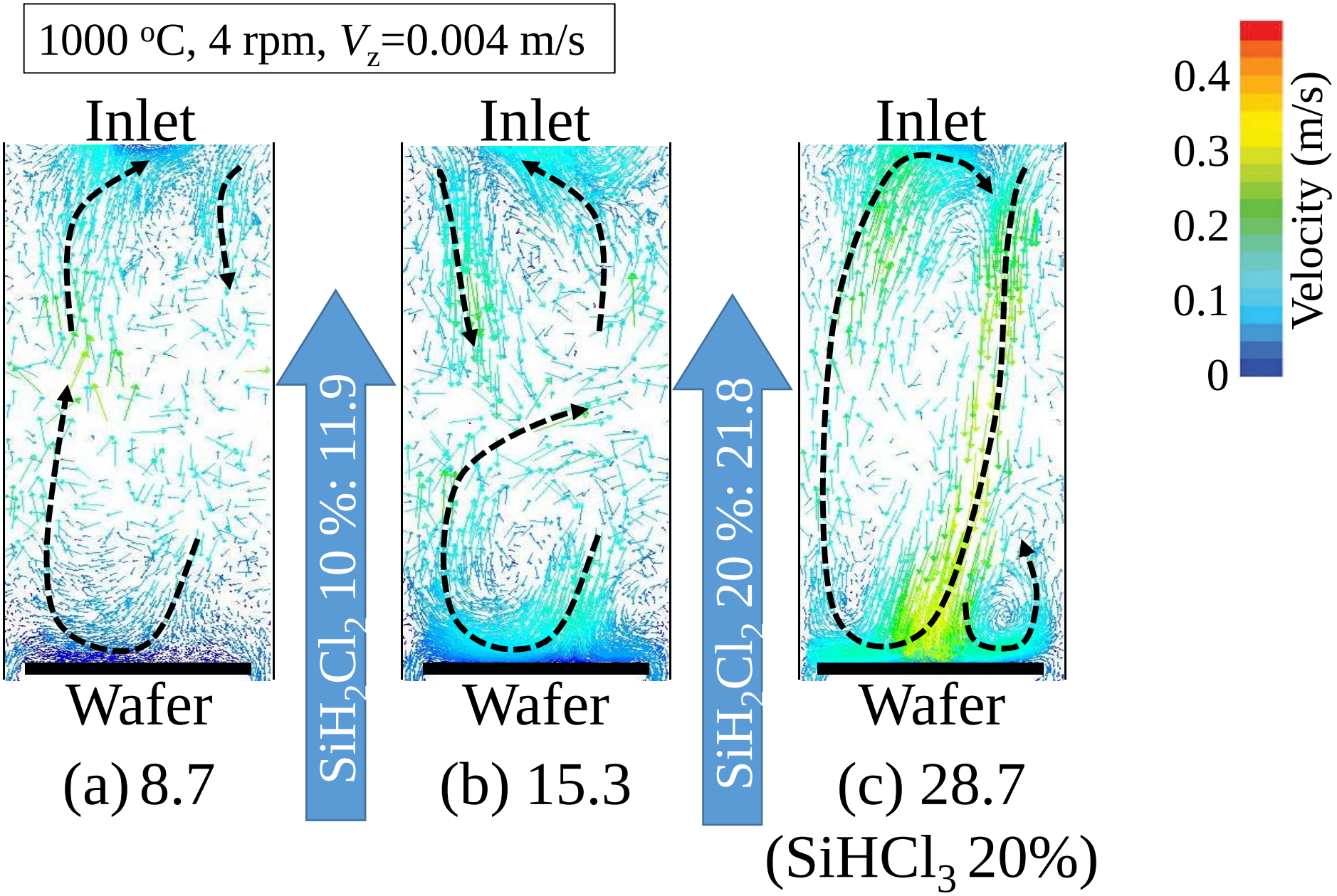
1000 °C, 4 rpm, V_z=0.004 m/s
Inlet
Inlet
Inlet
Wafer
Wafer
Wafer
SiH_2Cl_2 10 %: 11.9
SiH_2Cl_2 20 %: 21.8
(a) 8.7
(b) 15.3
(c) 28.7
($SiHCl_3$ 20%)
0.4
0.3
0.2
0.1
0
Velocity (m/s)

Figure 6

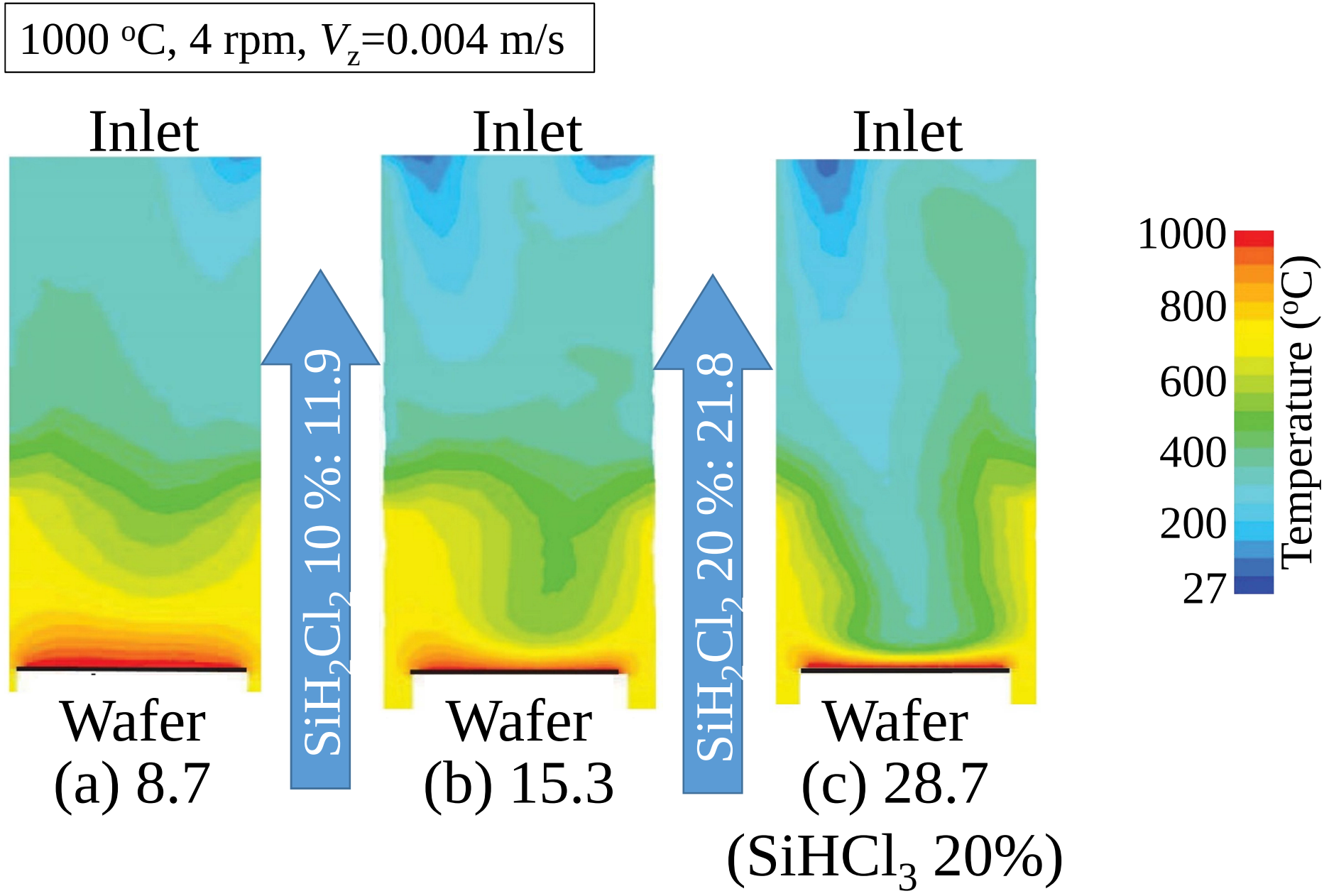
1000 °C, 4 rpm, V_z=0.004 m/s
Inlet
Inlet
Inlet
SiH_2Cl_2 10 %: 11.9
SiH_2Cl_2 20 %: 21.8
Wafer
(a) 8.7
Wafer
(b) 15.3
Wafer
(c) 28.7
($SiHCl_3$ 20%)
1000
800
600
400
200
27
Temperature (°C)

Figure 7

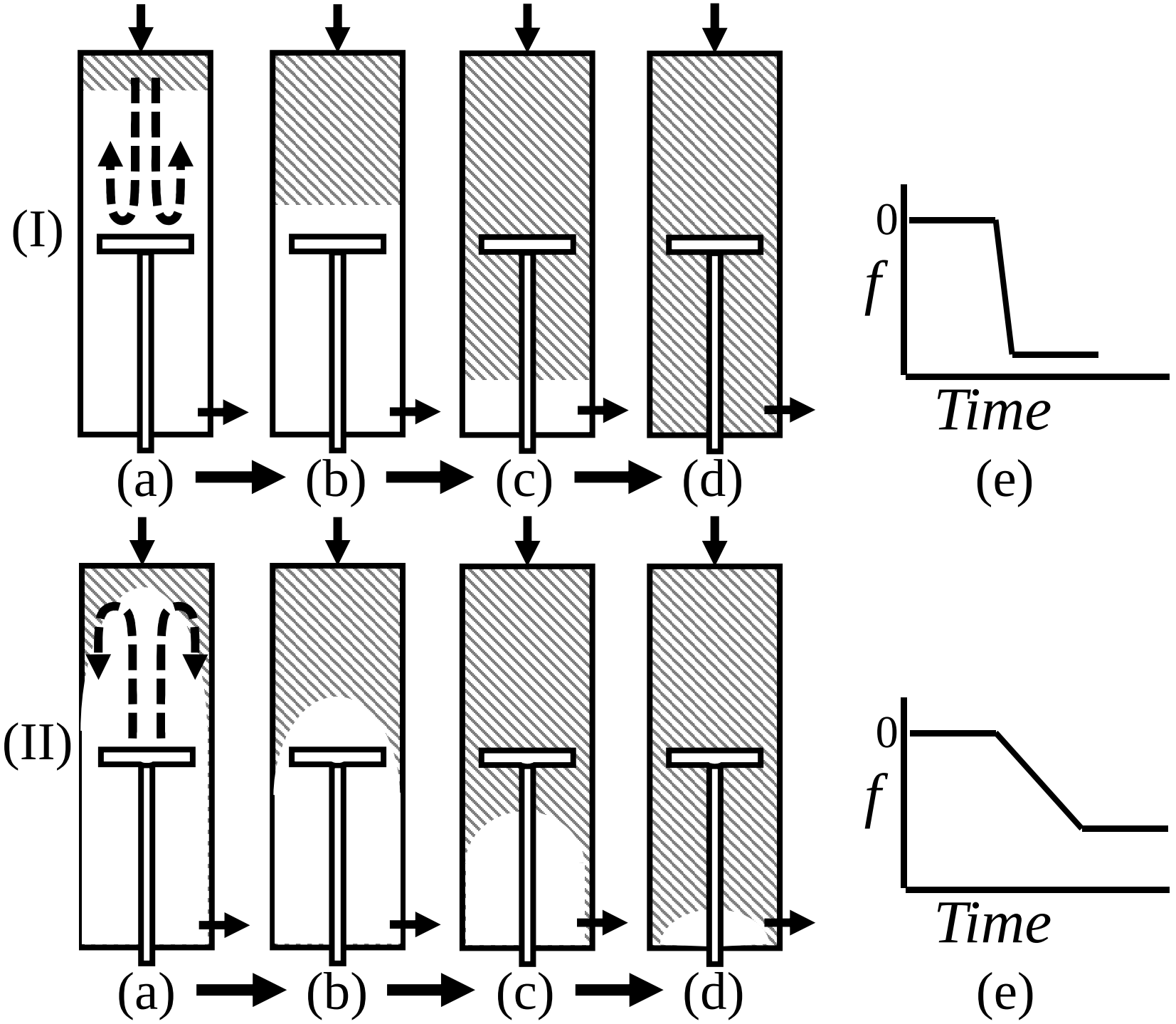

Figure 8